

Dear author,

Please note that changes made in the online proofing system will be added to the article before publication but are not reflected in this PDF.

We also ask that this file not be used for submitting corrections.



Contents lists available at ScienceDirect

Journal of Industrial and Engineering Chemistry

journal homepage: www.elsevier.com/locate/jiec1 Minimizing methanol content in experimental charentais alembic
2 distillations3 **Qi** Ricardo Luna^a, Francisco López^b, José R. Pérez-Correa^{a,*}4 ^aDepartamento de Ingeniería Química y Bioprocesos, Pontificia Universidad Católica de Chile, Vicuña Mackenna 4860, Casilla 306, Santiago 22, Chile5 ^bDepartament d'Enginyeria Química, Universitat Rovira i Virgili, Av. Països Catalans 26, 43007 Tarragona, Spain

ARTICLE INFO

Article history:

Received 27 June 2017

Received in revised form 9 August 2017

Accepted 11 August 2017

Available online xxx

Keywords:

Aromas

Distillation

Multi-objective optimization

Dynamic optimization

Spirits

Simulation

ABSTRACT

This study focuses on using modern engineering tools to consistently produce spirits with low methanol content in Charentais alembics. The method involves developing a dynamic model, formulating a multi-objective dynamic optimization problem, and implementing an automatic process control system. Optimization yielded a variable temperature in the partial condenser, which was tracked by an automatic control system that manipulated the heat addition in the boiler. The procedure was experimentally validated in triplicate using a ternary mixture. With the optimal operation, distillates with 12% less methanol than standard distillates were reproducibly obtained, with a moderate reduction (2.4%) in the ethanol recovery.

© 2017 The Korean Society of Industrial and Engineering Chemistry. Published by Elsevier B.V. All rights reserved.

6 **Introduction**

7 Distilled alcoholic beverages are produced worldwide from
8 local raw materials. For example, whisky (UK, Ireland) is produced
9 from cereals, cachaça from cane juice (Brazil), tequila from agave
10 (Mexico), cognac/brandy (France, Spain) and pisco (Peru, Chile)
11 from grapes [1]. Young distillates are characterized by a delicate
12 aroma that resembles the original fruit. In addition, high quality
13 spirits should be free from off-flavors and toxic compounds. In
14 spirits production processes, distillation plays a key role to ensure
15 that the standards of quality of the product are met. This is an
16 operation already used by ancient cultures to produce medicines
17 and perfumes, and nowadays are used in almost every chemical
18 processing plant. Distillation is a method for separating substances
19 of different volatility. Most spirits production processes use either
20 batch distillation columns or Charentais alembics. The latter are
21 most frequently used in small-scale production facilities. In this
22 system, three cuts (head, heart and tail) are collected sequentially;
23 high quality spirits are produced from the heart cut. Even though
24 the operation of alembics is relatively simple compared to batch
25 distillation columns, it is subjected to many uncontrolled and
26 unmeasured disturbances that generate variability in the

composition of the final product. Hence, it is still difficult to
ensure that the produced spirit consistently meets a defined
quality criterion. It is even more difficult to adapt the production
process to meet changing market trends.

There are many published studies dealing with the production
of fruit distillates in Charentais alembics and distillation columns
[2–9]. Many of these studies were concerned with the impact of the
fruit variety or the distillation equipment on the aroma composition
of the spirit. In addition, in these studies distillation strategies
were not changed and were defined heuristically. Recent studies
have explored the impact of different operating strategies on the
composition of Muscat wine distillates obtained in a packed batch
distillation column [10,11]. It was found by trial and error that low
reflux rates at the beginning of the heart cut could produce
distillates with an enhanced floral aroma. Although establishing
suitable alembic distillation strategies by trial and error is a valid
option that has been used for centuries in the production of spirits,
medicines and perfumes, these strategies can be developed much
faster and reliably using model based optimization [12,13].

Several techniques have long been applied to design optimal
operating strategies for batch distillation processes relevant in
chemical engineering. Most of these methods transform the usual
strategy design into an optimal control problem, where the usual
goals are to minimize time, maximize distillate, maximize
concentration of a key component or maximize profit [14,15]. As
a result, most of the time, difficult nonlinear programming problems
(NLP) should be solved numerically, either by the sequential

* Corresponding author.

E-mail addresses: rlluna@uc.cl (R. Luna), francisco.lopez@urv.cat (F. López),
perez@ing.puc.cl (J.R. Pérez-Correa).<http://dx.doi.org/10.1016/j.jiec.2017.08.018>

1226-086X/© 2017 The Korean Society of Industrial and Engineering Chemistry. Published by Elsevier B.V. All rights reserved.

(Intel® Core™ 2 Hewlett-Packard). A cascade control system was applied: the primary controller (outer loop) read the head temperature and provided the heating power set point for the secondary controller; the secondary controller (inner loop) adjusted the applied heating power to follow the set point provided by the primary controller. Both controllers used an internal model control (IMC) algorithm [39].

Experiments

In this study, a synthetic ternary mixture was prepared with a composition usually found in wine, i.e., 13% v/v of ethanol and 1.37 g/L.a.a. of methanol (grams of methanol per liter of absolute alcohol). The solution was prepared once and in sufficient amount before all the experimental distillations. The Alembic was initially loaded with 1.8 L of synthetic wine in each experiment. Distillation strategies were defined in terms of the heating power applied to the boiler. Three strategies (performed in triplicate) were assessed: (i) slow distillation at constant low heating power (230 W); (ii) fast distillation at constant high heating power (400 W); and (iii) optimal distillation applying a variable heating power. The first two strategies are common practice in small-scale spirits production facilities: slow distillations tend to increase spirits quality while fast distillations tend to increase ethanol recovery. The third strategy was defined to balance two objectives; low methanol content and high ethanol recovery (see section 2.7). In all distillation runs, three fractions were collected according to predefined volumes: 85 mL of head, 375 mL of heart and 115 mL of tail. The corresponding total distillation times were 168, 67 and 87 min for the slow, fast and optimal distillations respectively.

Chemical analysis

Ethanol content was determined (in triplicate) with a pycnometer, correcting the density to 20 °C. Methanol content was determined (in duplicate) using the method proposed by the International Organization of Vine and Wine (OIV) [40]. Distillate samples were diluted up to an ethanol content of 5% v/v and the methanol in the diluted samples was oxidized to formaldehyde with a solution of 3% w/v potassium permanganate and 15% v/v phosphoric acid. Then, the diluted oxidized samples were bleached with dry sodium bisulfite. The amount of formaldehyde was defined by the intensity of the violet color followed by the reaction of 5% w/w chromotropic acid in a sulfuric medium. This intensity was determined by spectrophotometry UV–vis (T70 UV/VIS spectrometer PG Instruments) at 575 nm. All reagents were analytical grade. We used these low cost analytical techniques instead of gas chromatography (GC) or high-pressure liquid chromatography (HPLC), since these are too expensive to be implemented in small-scale distilleries.

Data reconciliation

Total mass, alcoholic strength and methanol concentrations were measured in the synthetic wine initially charged in the boiler, in all the distillate samples and in the residue left in the boiler after distillation. Discrepancies were found in the global mass balances due to measurement errors. Therefore, measurements were corrected with a standard data reconciliation procedure normally applied in the process industries [41]. Hence, reconciled values closed the global mass balances (total mass, ethanol and methanol).

Modelling

A simplified version of the model presented in Sacher et al. [38] is used here, which considers a mixture of water, methanol and

ethanol. The model comprises total mass, ethanol and energy dynamic balances in the boiler, as well as total mass, ethanol and energy stationary balances in the partial condenser. Several constitutive equations were included to describe the heat loss to the environment and the vapor/liquid equilibrium. The complete model is given in Appendix A and further details and specific assumptions can be found in Sacher et al. [38].

Model calibration

The data obtained in the constant heat rate distillations (see Section 2.2) were used to calibrate the dynamic alembic model. The fitting parameters were:

$$\theta = [UA_b, UA_c, M_0, x_0^e, x_0^m] \quad (1)$$

where UA_b and UA_c represent the global heat transfer coefficient multiplied by the corresponding heat transfer area in the boiler and head respectively. M_0 , x_0^e and x_0^m are the initial total moles, ethanol molar fraction and methanol molar fraction in the boiler just at the moment when the first drop of distillate is recovered. These unmeasured values were different from those of the initial mixture. For the optimal strategy, the heat transfer parameters (UA) were not fitted; instead, they were modeled as linear functions of the heat transfer parameters fitted with the constant heating experiments.

The calibration cost function was:

$$J(\theta) = \sum_j \sum_{i=1}^{n_{\text{obs}}} \left(\frac{\hat{y}_{ij}(u, \theta, t) - y_{ij}(u, t)}{\max(y_{ij})} \right)^2 \quad (2)$$

where index j represents the measured variables and index i the sample times. The measured variables were: alcoholic strength GA , methanol concentration M_{eth} , distilled volume V and head temperature T_c . $\max(y_{ij})$ corresponds to the maximum measured value of variable j during the distillation run. The optimization problem was solved within MATLAB® R2015a with the scatter search metaheuristic code (SSM) [42].

Eqs. (A.20), (A.21) and (A.22) in Appendix A, that represent the instant concentration of ethanol, methanol and relative methanol respectively, were modified. Hence, Eqs. (3)–(5) represent the average concentration of the distillate stream leaving the system at the corresponding time interval where the sample was collected:

$$GA_i = \frac{\Delta GA}{\Delta V} = \left(\frac{M_D^e(t_{exp,i}) - M_D^e(t_{exp,i-1})}{V(t_{exp,i}) - V(t_{exp,i-1})} \right) \cdot PM_E \cdot \frac{1}{\rho_e} \cdot 100 \quad (3)$$

$$M_{et,i} = \frac{\Delta M_{et}}{\Delta V} = \left(\frac{M_D^m(t_{exp,i}) - M_D^m(t_{exp,i-1})}{V(t_{exp,i}) - V(t_{exp,i-1})} \right) \cdot PM_M \cdot 1 \cdot 10^{-6} \quad (4)$$

$$C_{meth,i} = \frac{\Delta C_{meth}}{\Delta V} = \left(\frac{M_D^m(t_{exp,i}) - M_D^m(t_{exp,i-1})}{(V(t_{exp,i}) - V(t_{exp,i-1})) \cdot (GA_i/100)} \right) \cdot PM_M \cdot 1000 \quad (5)$$

Finally, the heart cut of the three distillation strategies were compared. In model calibrations, the cut times of head/heart and heart/tail for each strategy were defined by the volumes collected, i.e., 85 mL of head and 375 mL of heart (see Section 2.2).

Dynamic optimization

A multi-objective cost function, $J(u)$, was defined to get a good compromise between low relative methanol concentration in the

distillate and high ethanol recovery.

$$\min_u J(u) = \alpha \cdot \frac{C_{meth}(t_f)}{1.5} - (1 - \alpha) \cdot \frac{Rec_{eth}(t_f)}{100} \quad (6)$$

here, α is an arbitrary positive scalar (≤ 1) that defines the relative weight of each objective [43,44] and C_{meth} is the relative methanol concentration. Ethanol recovery was defined by:

$$Rec_{eth} = \frac{\int_{t_0}^{t_f} (V_D(t) \cdot x_{eth}(t)) dt}{M_0 \cdot x_{eth}(t_0)} \quad (7)$$

where V_D is the molar flow rate of distillate, x_{eth} is the ethanol mole fraction, M_0 is the initial mass, and finally, t_0 and t_f are the initial and final distillation times respectively. Both objectives were scaled by their maximum values: the maximum methanol concentration in spirits allowed in the Chilean law [45] is 1.5 g/L.a.a, while the maximum ethanol recovery is 100%.

The only input variable that could be manipulated in the alembic was the heating power. Hence, the optimization problem looked for a heating path that minimized the relative methanol concentration in the distillate and simultaneously maximized ethanol recovery.

Only the heart cut was considered in computing the cost function (Eq. (6)). Based on experience, the head/heart cut was fixed at 5.5 min and the heart/tail cut was set at 120 min. Additional optimization constraints were: (i) the heating power varied between 230 and 400 W; (ii) the minimum distillate flow rate was 2 mL/min.

Two numerical methods were applied to solve the optimization problem [46]: the sequential solution/optimization method (SEM) and the simultaneous solution/optimization method (SIM). In SEM, the control variable was discretized into 18 equally spaced time steps where the control value was kept constant:

$$u(\Delta t_i) = a_i \quad (8)$$

where index i represents the 18 time intervals and a_i represents the value of the control u in the i -th time interval. The scatter search code mentioned above was used to solve the resulting optimization problem within MATLAB[®] R2015a. The dynamic model of the alembic was solved with MATLAB's solver *ode15s* [47]. In turn, in SIM, the control and state variables were discretized in time using

3 Radau collocation points on 18 finite elements [16,27]. The resulting optimal control problem was:

$$\min_u J(u) \quad (9)$$

Subject to,

$$\forall i = 1 \dots ne, j = 1 \dots ncp$$

$$x_{ij} = x_{i-1} + h_i \sum_{j=1}^{ncp} \Omega_j(\tau_j) \cdot \frac{dx}{dt_{ij}} \quad (10)$$

$$g(x_{ij}, y_{ij}, u_{ij}, \theta) = 0 \quad (11)$$

$$u_L \leq u_{ij} \leq u_U; x_L \leq x_{ij} \leq x_U; y_L \leq y_{ij} \leq y_U; \theta_L \leq \theta \leq \theta_U \quad (12)$$

$$\frac{dx}{dt_{ij}} = f(x_{ij}, y_{ij}, u_{ij}, \theta) \quad (13)$$

where ne represents the number of finite elements (18), ncp the number of collocation points (3), x the state variables, y the algebraic variables, u the control variables, θ the model parameters vector, h_i the length of the finite elements (total process time divided by the number of finite elements), and finally, Ω the interpolation polynomial functions in each finite element. The optimization problem was coded in AMPL [48] and solved with the IPOPT code [49].

Results

Model calibration

Figs. 2 and 3 show measured values and model outputs of the head temperature, alcoholic strength, methanol concentration, distillate volume and distillate flow rate of the three replicates of the constant high heating rate distillation. The 95% confidence intervals shown in the figures were obtained by simulation,

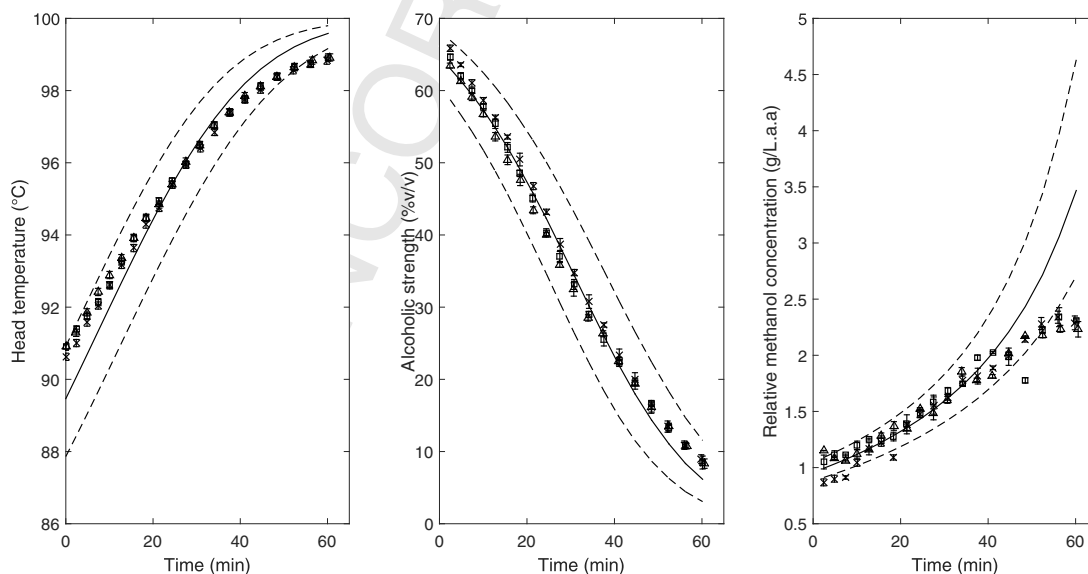


Fig. 2. Head temperature, alcoholic strength and relative methanol concentration for a constant heating power rate of 400 W. Experimental data: run 1 (\times), run 2 (\square) and run 3 (Δ). Simulation (solid line) and confidence interval (dashed line).

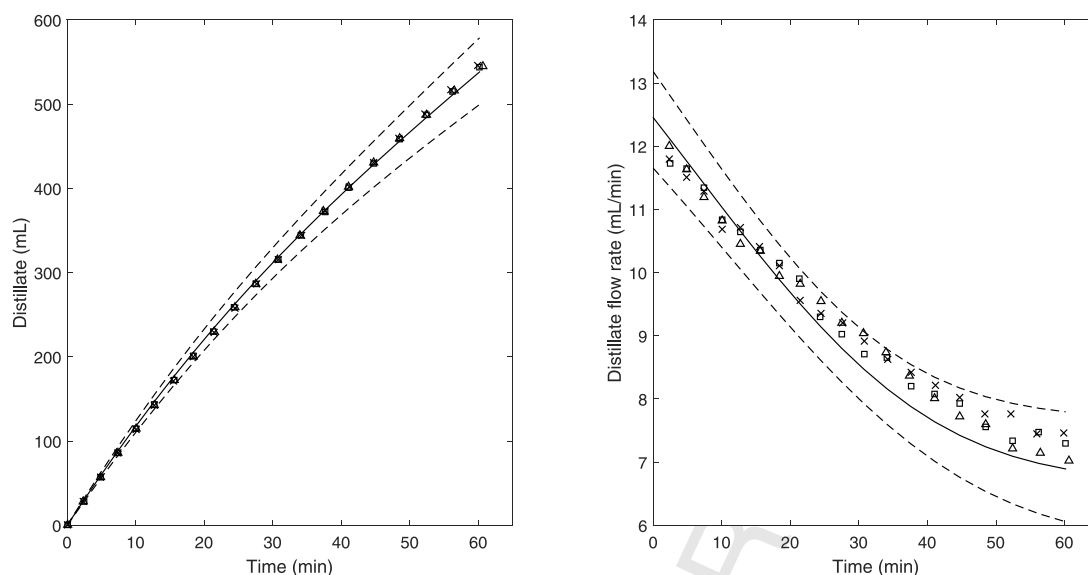


Fig. 3. Distillate volume and distillate flow rate for a constant heating power rate of 400 W. Experimental data: run 1 (\times), run 2 (\square) and run 3 (Δ). Simulation (solid line) and confidence interval (dashed line).

considering the standard deviation in the estimated parameter set ($\theta \pm 2\sigma_\theta$). Table 1 shows the fitted parameters for the two constant heating distillations (230 W and 400 W); for the optimal strategy, the initial concentrations were fitted only, since heat transfer parameters were defined by linear functions (see section 2.6).

Model fitting was better for the high heating rate distillation (Figs. 2 and 3) than for the low heating rate distillation (data not shown). At low heating, distillate flow rates were extremely low (less than 6 mL^{-1}) and distillation times were high (180 min); consequently, measurements were more sensitive to disturbances. The alcoholic strength and the distilled volume were the best-fitted variables in both distillation experiments. Simulated values did not represent well the measurements of relative methanol concentrations at the end of the distillation, especially for low heating operation (data not shown). In this case, low concentration and flow rate values were observed. Absolute errors of these measurements were approximately constant; hence, relative errors were higher at low concentration and flow rate values.

Table 1 shows that under low heating, the heat transfer parameters (UA) were practically the same for the boiler and the partial condenser. In turn, under high heating, the heat transfer parameter of the head was higher than that of the boiler. Sacher et al. [38] found the same behavior in a similar system; however, our heat transfer parameters were higher due to differences in the heating methods used. Sacher et al. [38] applied a hot plate to heat the boiler; hence, they could not measure the effective heat supplied, which was estimated instead. They argue also that low heating powers induced low convective air streams, reducing the heat transfer in the head. This explains why we observed a low heat transfer parameter of the head at low heating powers. The heat

transfer parameter of the boiler was less dependent on the heating power in our case, since the heating element is inside the boiler.

Optimal operation

Tables 2 and 3 show the optimization results with the SEM and SIM methods respectively, including the optimal values of relative methanol concentration (C_{meth}), ethanol and methanol recoveries ($Rec_{eth}, Rec_{C_{meth}}$), as well as alcohol strength (GA_d) for different values of the weight of the cost function ($0 \leq \alpha \leq 0.5$). For values of $\alpha \geq 0.5$, the same results were obtained, where the heating power was the lower limit. In the case of SIM, the optimization routine did not converge for some α values. Fig. 4 shows the optimum trajectories of the heating power, the head temperature and alcoholic strength variation for $\alpha = 0.05$ and $\alpha = 0.06$ obtained by SEM and SIM respectively. Fig. 5 shows the optimum trajectories of the heating power, the head temperature and alcoholic strength variation for $\alpha = 0.2$ obtained by SEM and SIM. Fig. 6 shows the Pareto front yielded by both dynamic optimization methods.

Both optimization methods provided different heating trajectories, where the SIM heating trajectories were easier to implement in real time experiments since they were much smoother. Even though different evolutions of head temperature and distillate alcoholic strengths were obtained for the same values of α , both methods yielded practically the same values of relative methanol concentration and ethanol recovery (Fig. 6, and Tables 2 and 3). Therefore, the optimal solutions found were reliable, since both methods, using different discretization techniques and optimization solvers, reached the same objective values. In addition, SEM was easier to apply than SIM, since the

Table 1
Fitted parameters for distillation strategies.

Strategy	UA_b ($\text{W}/^\circ\text{C}$)	UA_c ($\text{W}/^\circ\text{C}$)	M_0 (mol)	x_0^m (mol/mol)	x_0^n (mol/mol)
230 W	0.82 ± 0.06	0.81 ± 0.10	90.4 ± 1.2	$37.1\text{e-}3 \pm 0.7\text{e-}3$	$10.12\text{e-}5 \pm 0.13\text{e-}5$
400 W	0.37 ± 0.10	1.48 ± 0.13	90.4 ± 0.9	$38.5\text{e-}3 \pm 2.0\text{e-}3$	$10.41\text{e-}5 \pm 0.16\text{e-}5$
Optimal	^a	^b	89.5 ± 1.7	$36.6\text{e-}3 \pm 1.4\text{e-}3$	$9.40\text{e-}5 \pm 0.53\text{e-}5$

^a Linear function between UA_b values obtained from 230 and 400 W.

^b Linear function between UA_c values obtained from 230 and 400 W.

Table 2

Results obtained with the sequential solution/optimization method for head/heart cut at 5 min and heart/tail cut at 120 min.

Adjustable weight (α)	Objective function (J)	Relative methanol concentration (C_{meth})	Ethanol recovery (Rec_{eth})	Methanol recovery (Rec_{meth})	Alcohol strength (GA_d)
0	-0.915	1.40	91.5	94.3	24.8
0.05	-0.823	1.40	91.5	94.1	26.7
0.10	-0.730	1.39	91.4	93.5	29.9
0.15	-0.638	1.38	91.4	92.8	32.0
0.20	-0.547	1.37	91.2	91.9	34.2
0.25	-0.456	1.36	91.0	90.9	36.1
0.30	-0.365	1.35	90.6	89.5	38.2
0.35	-0.276	1.33	90.2	88.2	40.0
0.40	-0.186	1.31	89.5	86.3	42.0
0.45	-0.0985	1.30	88.5	84.2	44.1
0.50	-0.0116	1.27	86.7	80.5	47.1

Table 3

Results obtained with the simultaneous solution/optimization method for head/heart cut at 5 min and heart/tail cut at 120 min.

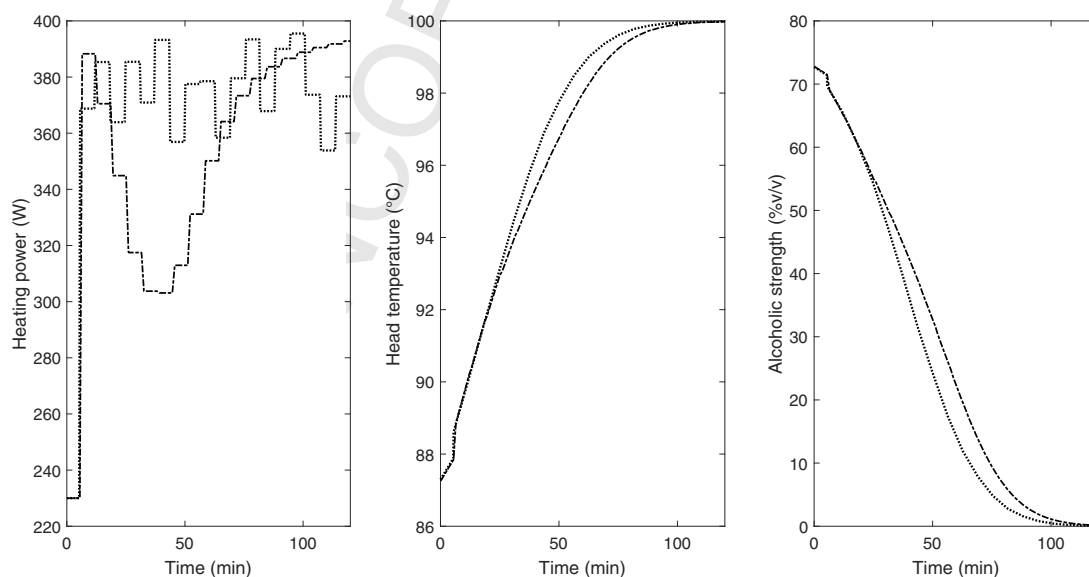
Adjustable weight (α)	Objective function (J)	Relative methanol concentration (C_{meth})	Ethanol recovery (Rec_{eth})	Methanol recovery (Rec_{meth})	Alcohol strength (GA_d)
0.06	-0.805	1.40	91.5	94.0	27.6
0.10	-0.731	1.39	91.5	93.5	29.9
0.15	-0.639	1.38	91.4	92.8	32.4
0.20	-0.547	1.37	91.2	91.9	34.5
0.25	-0.456	1.36	91.0	90.8	36.6
0.30	-0.366	1.35	90.7	89.6	38.5
0.36	-0.258	1.33	90.1	87.8	40.8
0.40	-0.187	1.31	89.5	86.3	42.4
0.43	-0.134	1.30	89.0	85.1	43.6
0.45	-0.0987	1.29	88.6	84.2	44.4
0.48	-0.0465	1.28	87.8	82.7	45.6
0.50	-0.0120	1.27	87.2	81.5	46.5

model was already coded in MATLAB[®] and the DAE system was efficiently solved with the *ode15s* routine. Therefore, we only had to add the optimization routine, code the multi-objective cost function and discretize the control variable. For the SIM approach, the code was adapted to AMPL language (which was rather difficult) and the model was fully discretized, generating many equations, variables and inequality constraints in the state variables and the control variable.

SEM solved the optimization problem much slower than SIM (5–10 h for SEM and 1–5 s for SIM). The SEM approach solved the

numerical integration of the DAE system at each iteration step. Instead, SIM solved the optimization problem once at the optimal point. However, in many cases the SIM method could not solve the optimization problem since the model did not converge due to numerical limitations.

For $\alpha = 0.06$ for SEM and 0.05 for SIM, the high-limit heating rate (400 W) was obtained, resulting in the highest ethanol recovery (objective 1) at the expense of the highest methanol concentration (objective 2). In turn, for $\alpha \geq 0.5$, the low-limit heating rate (230 W) was obtained, yielding the lowest ethanol recovery and lowest

**Fig. 4.** Heating power, head temperature and instant alcoholic strength optimal curves obtained by SEM ($\alpha = 0.05$, dotted line) and SIM ($\alpha = 0.06$, dash-dot line).

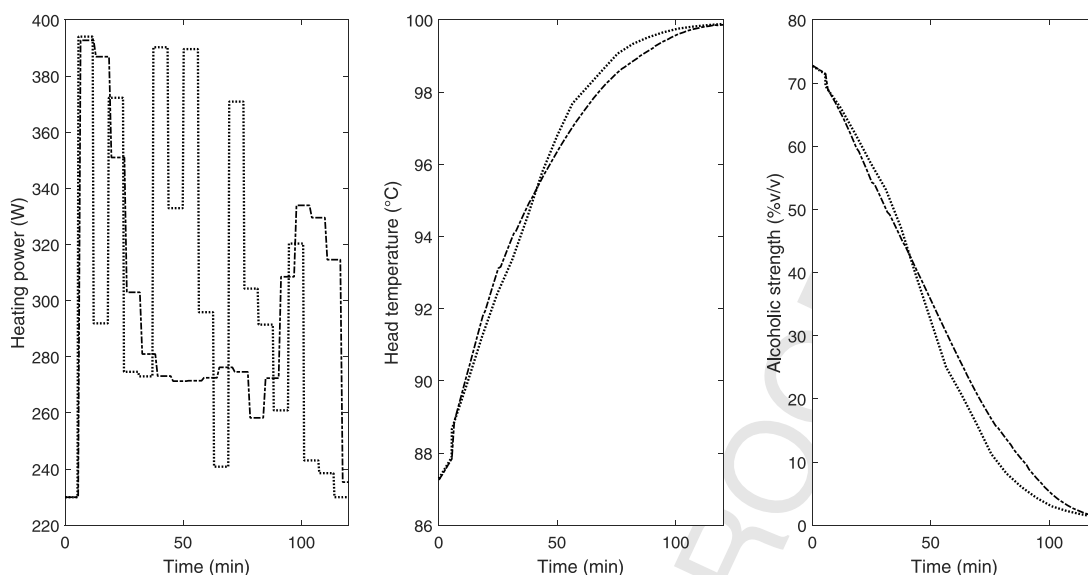


Fig. 5. Heating power, head temperature and instant alcoholic strength optimal curves obtained by $\alpha=0.2$. SEM (dotted line) and SIM (dash-dot line).

372 methanol concentration. In this case, it was possible to reduce the
373 relative methanol concentration 7.3% compared to the concentra-
374 tion in the initial mixture (1.37 g/L.a.a.), recovering 87.2% of the
375 ethanol (Table 3). De Lucca et al. [35] were able to reduce the
376 relative methanol concentration in the distillate by 22.7% in
377 relation to the initial mixture, recovering 75% of the ethanol in a
378 simulated packed column. In addition, these authors observed that
379 smaller head/heart and heart/tail cut times yielded lower
380 methanol concentrations, independently of the distillation strategy.
381 Thus, to compare both distillation methods (Charentais alembic
382 and packed distillation column) in their ability to reduce the
383 distillate methanol content, we solved the optimization problem
384 with $\alpha=1$, reducing the head/heart cut time and fixing the ethanol
385 recovery at 75%. We were able to reduce the methanol content in
386 the distillate by 16.8% (1.14 g/L.a.a) in relation to the initial mixture.
387 A batch packed column distillation system has a much higher
388 rectification capacity than a Charentais alembic; therefore, it can
389 reduce the methanol concentration in the distillate 35% more than
390 the Charentais alembic.

Experimental validation

391
392 A good compromise between both optimization objectives was
393 achieved with $\alpha=0.2$, where the methanol concentration was
394 below the legal limit without sacrificing ethanol recovery. Hence,
395 we performed the validation experiments (in triplicate) with this
396 solution, using the SIM head temperature as a variable set point to
397 be tracked by the control system. Fig. 7 shows the temperature set
398 point (optimal path), the measured head temperature, the room
399 temperature (disturbance) and the heating power (manipulated
400 variable).

401 The measured head temperature evolutions were the same in
402 the three experimental runs, closely tracking the optimal path
403 despite the different evolutions of the room temperature. Small
404 variations in the manipulated variable efficiently compensated
405 these disturbances. It is worth noticing that the optimal experi-
406 ment finished earlier than predicted by the model. In the
407 experiments, the cuts were defined by the recovered volumes,
408 in order to simplify the comparison with the constant heating

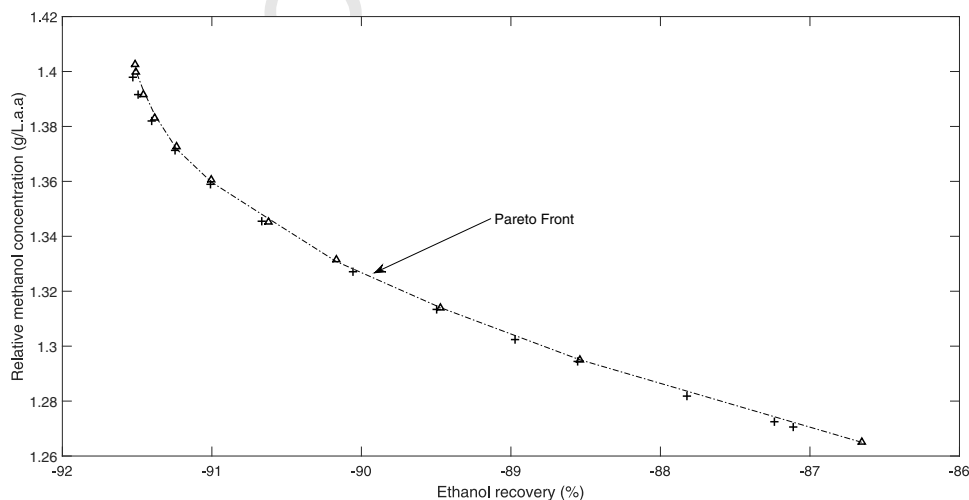


Fig. 6. Relative methanol concentration (objective 1) vs ethanol recovery (objective 2). Sequential method (Δ) and simultaneous method (+).

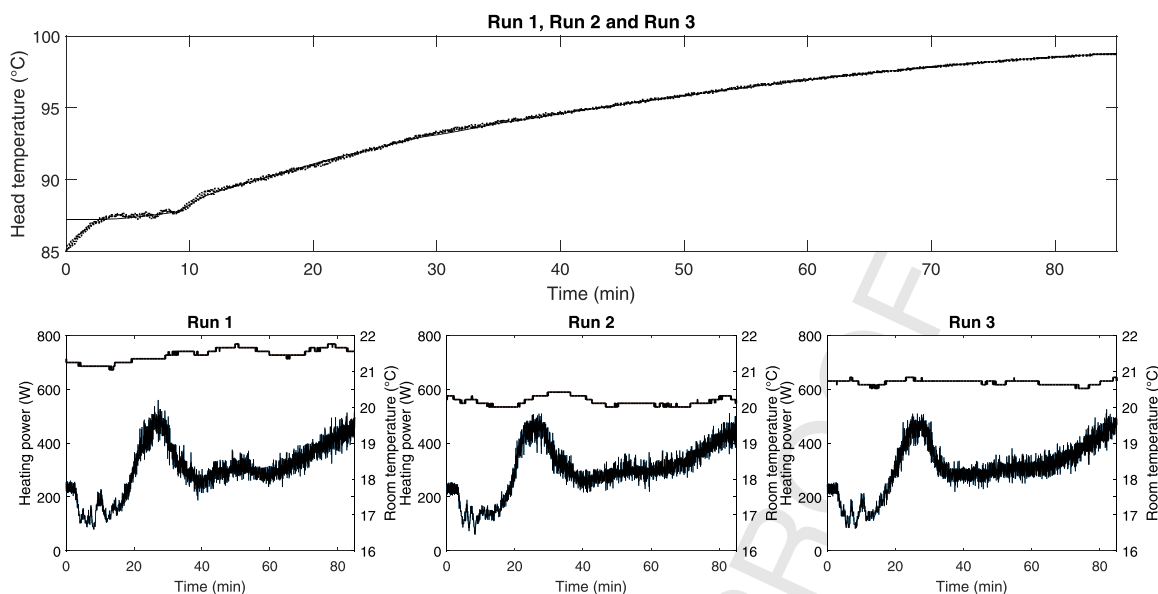


Fig. 7. Experimental optimal strategy in triplicate. Top figure: head temperature set point (solid line) and measured temperatures (dotted lines). Bottom figures: room temperature (thin lines) and heating power (thick lines).

strategies (see Section 2.2). Moreover, the final distillate corresponds to the tail fraction cut which was not part of the optimization objective.

Figs. 8 and 9 show a good agreement between simulations and measured values, where most of them lie within the confidence interval. Like in the model calibration experiments, alcoholic strength and distilled volume were the best-fitted variables.

We compared the heart cut ethanol recovery and relative methanol concentration obtained in the three distillation strategies. Simulations of all strategies considered 85 mL of head and 375 mL of heart (see Section 2.2), and these were compared with experimental values (Fig. 10). Experiments confirmed that the optimal strategy achieved the lowest methanol concentration in the heart cut (1.23 g/L.a.a.).

The experimental relative methanol concentrations were practically the same for high and low heating power strategies,

while simulated values (based on cut times) were significantly different (see Tables 2 and 3). In the experiments, for simplicity, the fractions were defined by volume, while in the simulations the fractions were defined by fixed cut times. Nevertheless, simulations of methanol concentrations in the heart fractions based on volumes were quite accurate in all experiments (see Fig. 10). Simulations of ethanol recovery were inaccurate only for the optimal heating strategy, which was overestimated by 9%. This overestimation can be due to differences between simulated and experimental heating, where the latter covered a wider range of values (0–500 W) to provide the control system more flexibility to cope with unmeasured disturbances. In addition, our model included several approximations regarding the energy balances: (i) the heat transfer parameters in the optimal strategy (UA) were a linear function of the heating power applied in the boiler between 230–400 W; (ii) the energy balances did not consider the thermal

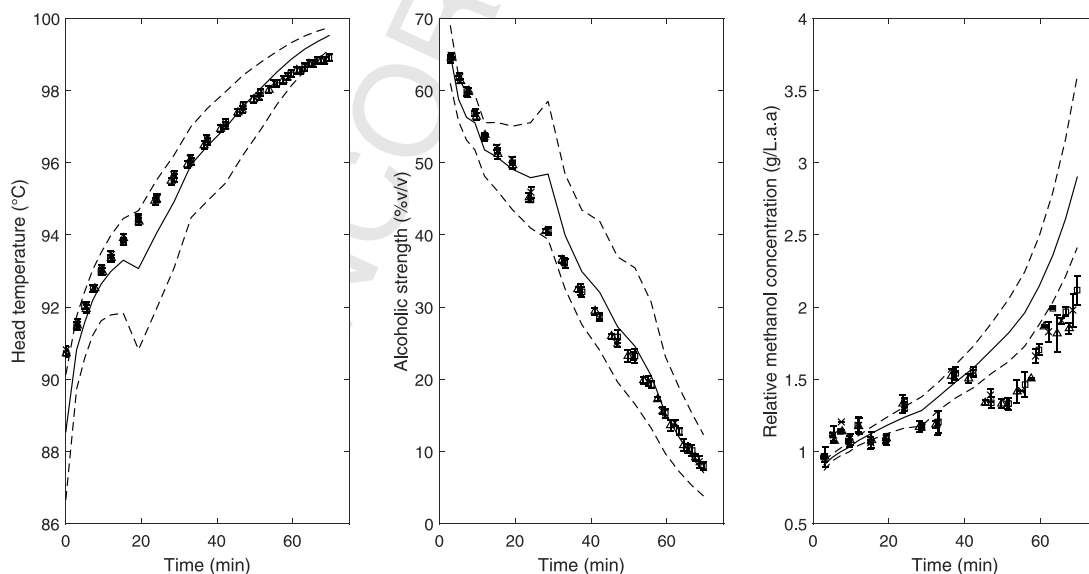


Fig. 8. Experimental optimal strategy: head temperature, alcoholic strength and methanol concentration. Experimental data: run 1 (\times), run 2 (\square) and run 3 (Δ). Simulation (solid line) and confidence interval (dashed line).

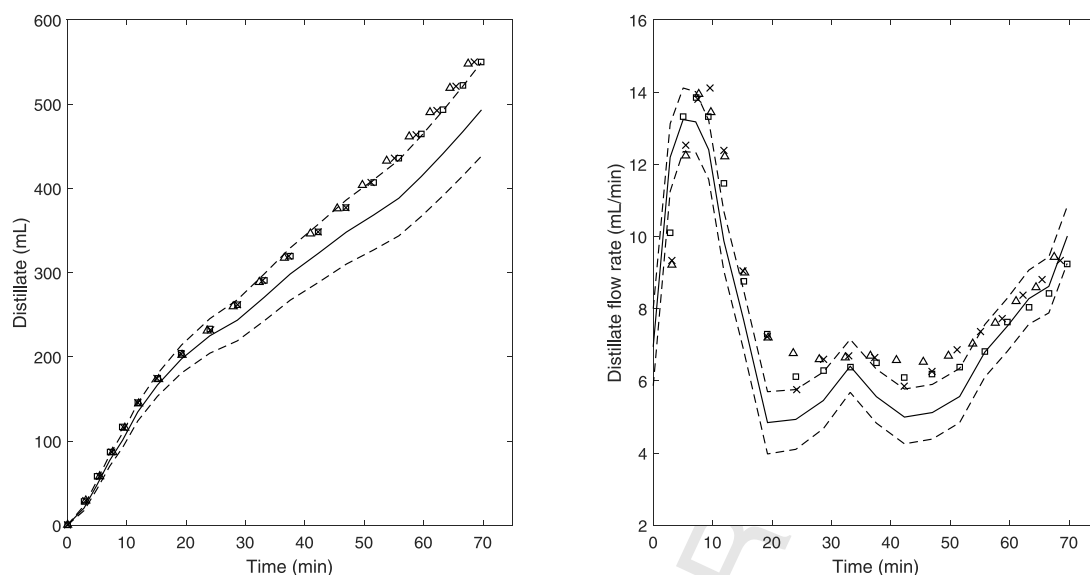


Fig. 9. Experimental optimal strategy: distillate volume and distillate flow rate. Experimental data: run 1 (x), run 2 (□) and run 3 (Δ). Simulation (solid line) and confidence interval (dashed line).

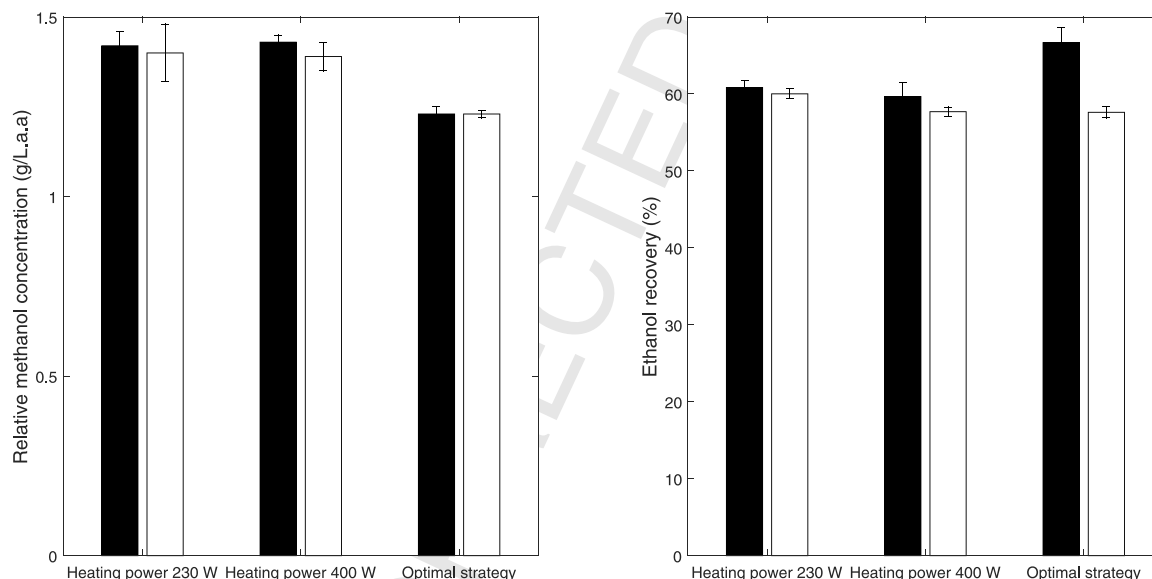


Fig. 10. Relative methanol concentration and ethanol recovery in the heart cut for each distillation strategy: predicted values (■) and experimental data (□).

441 inertia contribution of the 2.5 kg of copper of the alembic; and (iii)
442 the accumulation term in the energy balance in the head of the
443 alembic (partial condenser) was neglected. Since ethanol content
444 in the distillate depends strongly on the equilibrium temperature
445 and varied widely in all distillation runs (between 5 and 65%),
446 simulations of the heart cut ethanol recovery were quite sensitive
447 to the small errors in the simulated instantaneous values due to the
448 assumptions above. In turn, relative methanol concentrations were
449 less dependent on the equilibrium temperature and varied in a
450 much narrower range (between 1.23 and 1.45); hence, those small
451 errors due to the energy balance assumptions had much less
452 impact on the predictions of the relative methanol concentration
453 in the heart cut. Nevertheless, by applying the methodology
454 described above, we were able to reproducibly obtain in
455 experimental runs a distillate with 12% less methanol than
456 standard strategy distillates, with a moderate reduction (2.4%)
457 in the ethanol recovery.

458 Conclusions

459 A reliable method was presented to develop optimal operating
460 strategies for Charentais alembics that simultaneously achieved
461 high ethanol recoveries and low methanol concentrations in the
462 distillate. The developed model accurately reproduced the
463 experimentally observed methanol concentrations in the optimal
464 strategy. Experimental ethanol recoveries were 9% lower than
465 simulated for the optimal strategy, due to model approximations
466 and the wider operating range of the control variable of the
467 experimental system. With the optimal strategy tested experi-
468 mentally, we were able to reduce the methanol concentration in
469 the distillate by 12% compared with standard operating strategies
470 (constant heating rates), without a significant reduction in the
471 ethanol recovery. In particular, our results showed that a volatile
472 impurity such as methanol could be reduced in the spirit by
473 applying a low heating power during the head cut. In addition,

increasing the heating power at the beginning of the heart cut will favor the recovery of ethanol. Much better distilled spirits can be obtained by applying model-based engineering tools than those achieved by trial and error experimentation or intuitively. In addition, the methodology proposed in this study could be easily applied to tackle objectives that are more challenging. For example, to produce spirits with enhanced floral aroma and reduced off-flavors. This technology can be applied in small and medium distilleries since the system implementation is relatively simple and low cost.

Acknowledgements

Ricardo Luna appreciates a PhD scholarship from CONICYT PAI/INDUSTRIA79090016. We are grateful to Lisa Gingles who review the English style of the manuscript.

Appendix A. Alembic model

Mass (total, ethanol, methanol) and energy balances in the boiler,

$$\frac{d(M_B)}{dt} = L - V_B \quad (\text{A.1})$$

$$\frac{d(M_B \cdot x_B^e)}{dt} = L \cdot x_L^e - V_B \cdot y_B^e \quad (\text{A.2})$$

$$\frac{d(M_B \cdot x_B^m)}{dt} = L \cdot x_L^m - V_B \cdot y_B^m \quad (\text{A.3})$$

$$\frac{d(M_B \cdot u_B)}{dt} = L \cdot h_L - V_B \cdot H_B + \dot{Q}_B \quad (\text{A.4})$$

Mass (total, ethanol, methanol) and energy balances in the partial condenser (negligible liquid holdup),

$$V_B - L - V_D = 0 \quad (\text{A.5})$$

$$V_B \cdot y_B^e - L \cdot x_L^e - V_D \cdot y_D^e = 0 \quad (\text{A.6})$$

$$V_B \cdot y_B^m - L \cdot x_L^m - V_D \cdot y_D^m = 0 \quad (\text{A.7})$$

$$V_B \cdot H_B - L \cdot h_L - V_D \cdot H_D - \dot{Q}_C = 0 \quad (\text{A.8})$$

Thermodynamic equilibrium relationships for methanol,

$$y_D^m = K_C^m \cdot x_L^m \quad (\text{A.9})$$

$$y_B^m = K_B^m \cdot x_B^m \quad (\text{A.10})$$

$$K_{B,C}^m(x_B^e, x_L^e) = \frac{y_{B,D}^m}{x_{B,L}^m} = \frac{P_m(x_B^e, x_L^e) \cdot \gamma_m(x_B^e, x_L^e)}{P} \quad (\text{A.11})$$

The activity coefficient for methanol γ_m is estimated using the UNIFAC contribution groups method. Given the assumption of a quasi-binary mixture, the activity coefficient only depends on the ethanol concentration since an infinite dilution of methanol in a mixture of water-ethanol is assumed.

Heat transfer model

$$\dot{Q}_B = \dot{Q}_{cal} - UA_b \cdot (T_B - T_{env}) \quad (\text{A.12})$$

$$\dot{Q}_C = UA_c \cdot (T_C - T_{env}) \quad (\text{A.13})$$

Where \dot{Q}_{cal} and T_{env} are input variables corresponding to the control variable and disturbance of the system respectively. This model has only one empirical parameter, $U \cdot A$, which can be easily fitted with data normally available in commercial distillation facilities [50].

Simulation

To simulate the model, a reordering of equations is convenient. The distillate molar flow rate is obtained from mass and energy balances in the partial condenser (Eqs. (A.5), (A.6) and (A.8))

$$V_D = \frac{\dot{Q}_C}{(H_B - H_D) + \frac{(y_B^e - y_D^e)}{(x_L^e - y_D^e)} \cdot (H_D - h_L)} - \frac{\dot{Q}_C}{(h_L - H_D) + \frac{(x_L^e - y_D^e)}{(y_B^e - y_D^e)} \cdot (H_D - H_B)} \quad (\text{A.14})$$

To calculate the volume of distillate, an empirical correlation which calculates the density of the mixture from ethanol composition is used [51],

$$\rho_L(y_D^e) = \frac{y_D^e \cdot PM_E + (1 - y_D^e) \cdot PM_W}{\phi \cdot y_D^e + (1 - y_D^e) \cdot PM_W / \rho_W} \quad (\text{A.15})$$

$$\phi = f(y_D^e, T_D) \quad (\text{A.16})$$

To simulate the model outputs, the distilled volume (V), as well as the accumulated ethanol and methanol, must be calculated by three differential equations.

$$\frac{dV}{dt} = \frac{V_D \cdot (y_D^e \cdot PM_E + (1 - y_D^e) \cdot PM_W)}{\rho_L(y_D^e)} \quad (\text{A.17})$$

$$\frac{dM_D^e}{dt} = y_D^e \cdot V_D \quad (\text{A.18})$$

$$\frac{dM_D^m}{dt} = y_D^m \cdot V_D \quad (\text{A.19})$$

where M_D^e and M_D^m are the ethanol and methanol moles in the accumulated distillate, respectively. However, the ethanol concentration was measured in alcoholic strength (GA), the methanol concentration in mg/L (M_{eth}) and relative methanol concentration in g/L.a.a (C_{meth}).

$$GA = \frac{M_D^e \cdot PM_E \cdot (1/\rho_E)}{V} \cdot 100 \quad (\text{A.20})$$

$$M_{eth} = \frac{M_D^m \cdot PM_M}{V} \cdot 1 \cdot 10^{-6} \quad (\text{A.21})$$

$$C_{meth} = \frac{M_D^m \cdot PM_M}{V \cdot (GA/100)} \cdot 1000 \quad (\text{A.22})$$

Finally, to calculate the composition of ethanol in the partial condenser, a rearrangement of the energy balance (Eq. (A.4)) from

mass balances in the boiler (Eqs. (A.1) and (A.2)) is required,

$$\begin{aligned} & (L(x_L^e - x_B^e) - V_B(y_B^e - x_B^e)) \left(\frac{\partial h_B}{\partial x_B} + \frac{\partial h_B dT_B}{\partial T_B dx_B} \right) \\ & = L(h_L - h_B) - V_B(H_B - h_B) + \dot{Q}_B \end{aligned} \quad (\text{A.23})$$

This equation is an implicit function that depends on the value of x_L^e . This equation was solved iteratively using MATLAB's *fsolve* routine (in the sequential method) and in the AMPL code was included as an additional constraint in the optimization problem (in the simultaneous method).

References

- [1] R.W. Small, M. Couturier, M. Godfrey, *Beverage Basics: Understanding and Appreciating Wine, Beer, and Spirits*, Wiley, 2011.
- [2] Y. Arrieta-Garay, L. García-Llobodanin, J.R. Pérez-Correa, C. López-Vázquez, I. Orriols, F. López, *J. Agric. Food Chem.* 61 (2013) 4936.
- [3] Y. Arrieta-Garay, C. López-Vázquez, P. Blanco, J.R. Pérez-Correa, I. Orriols, F. López, *J. Inst. Brew.* 120 (2014) 111.
- [4] Y. Arrieta-Garay, P. Blanco, C. López-Vázquez, J.J. Rodríguez-Bencomo, J.R. Pérez-Correa, F. López, I. Orriols, *J. Agric. Food Chem.* 62 (2014) 10552.
- [5] M.J. Claus, K.A. Berglund, *J. Food Process Eng.* 28 (2005) 53.
- [6] C. Da Porto, D. Decorti, *Int. J. Food Sci. Technol.* 43 (2008) 638.
- [7] L. García-Llobodanin, J. Roca, J.R. López, J.R. Pérez-Correa, F. López, *Int. J. Food Sci. Technol.* 46 (9) (2011) 1956.
- [8] L.F. Hernández-Gómez, J. Úbeda, A. Briones, *Food Chem.* 82 (2003) 539.
- [9] R.V. Reche, A.F.L. Neto, A.A. Da Silva, C.A. Galinaro, R.Z. De Osti, D.W. Franco, *J. Agric. Food Chem.* 55 (2007) 6603.
- [10] P. Matias-Guiu, J.J. Rodríguez-Bencomo, I. Orriols, J.R. Pérez-Correa, F. López, *Food Chem.* 213 (2016) 40.
- [11] J.J. Rodríguez-Bencomo, J.R. Pérez-Correa, I. Orriols, F. López, *Food Bioprocess Technol.* 9 (2016) 1885.
- [12] D. Osorio, J.R. Pérez-Correa, L.T. Biegler, E. Agosin, *J. Agric. Food Chem.* 53 (16) (2005) 6326.
- [13] J. Sacher, L. García-Llobodanin, F. López, H. Segura, J.R. Pérez-Correa, *Chem. Eng.* 910 (2017) 32.
- [14] U. Diwekar, *Batch Distillation: Simulation, Optimal Design, and Control*, Taylor & Francis, 1995.
- [15] I.M. Mujtaba, *Batch Distillation: Design and Operation*, Imperial College Press, 2004.
- [16] S. Kameswaran, L.T. Biegler, *Comput. Chem. Eng.* 30 (2006) 1560.
- [17] P.I. Barton, R.J. Allgor, W.F. Feehery, S. Galán, *Ind. Eng. Chem. Res.* 37 (97) (1998) 966.
- [18] V.S. Vassiliadis, R.W.H. Sargent, C.C. Pantelides, *Ind. Eng. Chem. Res.* 33 (1994) 2111.
- [19] V.S. Vassiliadis, R.W.H. Sargent, C.C. Pantelides, *Ind. Eng. Chem. Res.* 33 (1994) 2123.
- [20] Y. Han Kim, *Chem. Eng. Process.* 38 (1999) 61.
- [21] S. Jain, J.K. Kim, R. Smith, *Ind. Eng. Chem. Res.* 51 (2012) 5749.
- [22] I.M. Mujtaba, S. Macchietto, *Comput. Chem. Eng.* 17 (12) (1993) 1191.
- [23] I.M. Mujtaba, S. Macchietto, *Ind. Eng. Chem. Res.* 36 (1997) 2287.
- [24] J.S. Logsdon, U.M. Diwekar, L.T. Biegler, *Chem. Eng. Res. Des.* 68 (1990) 434.
- [25] I.M. Mujtaba, S. Macchietto, *J. Process Control* 6 (1) (1996) 27.
- [26] L.T. Biegler, A.M. Cervantes, A. Wächter, *Chem. Eng. Sci.* 57 (2002) 575.
- [27] L.T. Biegler, *Chem. Eng. Process.* 46 (2007) 1043.
- [28] J.C. Zavala, C. Coronado, *Ind. Eng. Chem. Res.* 47 (2) (2008) 2788.
- [29] S.M. Safdarnejad, J.R. Gallacher, J.D. Hedengren, *Comput. Chem. Eng.* 86 (2016) 18.
- [30] P. Li, H.A. Garcia, G. Wozny, E. Reuter, *Ind. Eng. Chem. Res.* 37 (97) (1998) 1341.
- [31] S. Elgue, L. Prat, M. Cabassud, J.M. Le Lann, J. Cézerac, *Comput. Chem. Eng.* 28 (2004) 2735.
- [32] A. Bonsfills, L. Puigjaner, *Chem. Eng. Process.* 43 (2004) 1239.
- [33] C. Noeres, K. Dadhe, R. Gesthuisen, S. Engell, A. Górak, *Chem. Eng. Process.* 43 (2004) 421.
- [34] D. Osorio, R. Pérez-Correa, A. Belancic, E. Agosin, *Food Control* 15 (7) (2004) 515.
- [35] F. De Lucca, R. Munizaga-Miranda, D. Jopia-Castillo, C.A. Gelmi, J.R. Pérez-Correa, *Int. J. Food Eng.* 9 (3) (2013) 259.
- [36] J. Carvallo, M. Labbe, J.R. Pérez-Correa, C. Zaror, J. Wisniak, *Food Control* 22 (8) (2011) 1322.
- [37] R. Swift, D. Davidson, *Alcohol Health Res. World* 22 (1) (1998) 54.
- [38] J. Sacher, L. García-Llobodanin, F. López, H. Segura, J.R. Pérez-Correa, *Food Bioprod. Process.* 91 (4) (2013) 447.
- [39] C. Brosilow, B. Joseph, *Techniques of Model-Based Control*, Prentice Hall, 2002.
- [40] International Organisation of Vine and Wine, *Compendium of International Methods of Analysis-OIV: Methanol, Method OIV-MA-AS312-03B*, International Organisation of Vine and Wine, 2009.
- [41] S. Narasimhan, C. Jordache, *Data Reconciliation and Gross Error Detection: An Intelligent Use of Process Data*, Gulf Professional Publishing, 2000.
- [42] J.A. Egea, M. Rodríguez-Fernández, J.R. Banga, R. Martí, *J. Glob. Optim.* 37 (2007) 481.
- [43] V. Bhaskar, S.K. Gupta, A.K. Ray, *Rev. Chem. Eng.* 16 (2000) 1.
- [44] K. Miettinen, J. Hakanen, *Multi-Objective Optimization: Techniques and Applications in Chemical Engineering*, Mcdm, 2009, pp. 153.
- [45] Biblioteca del congreso nacional de Chile, Ministerio de Agricultura, *Reglamentación Ley N (18.455 que fija normas sobre producción, elaboración y comercialización de alcoholes etílicos, bebidas alcohólicas y vinages, (2012)*.
- [46] B. Srinivasan, D. Bonvin, E. Visser, S. Palanki, *Comput. Chem. Eng.* 27 (2003) 27.
- [47] L.F. Shampine, M.W. Reichelt, *SIAM J. Sci. Comput.* 18 (1) (1997) 1.
- [48] R. Fourer, D.M. Gay, B.W. Kernighan, (2003) 519.
- [49] A. Waechter, L.T. Biegler, On the implementation of a primal-dual interior point filter line search algorithm for large-scale nonlinear programming, *Math. Program.* 106 (2006) 25.
- [50] J.R. Pérez-Correa, R. Luna-Hernández, D. Jopia, S. Díaz, F. Huerta, F. López, XII Congreso de los Grupos de Investigación Enológica (Gienol), Madrid, 2013 p. 8.
- [51] H.J. Neuburg, J.R. Pérez-Correa, *Lat. Am. Appl. Res.* 24 (1) (1994) 1.